

Deep Learning-Optimized CLAHE for Contrast and Color Enhancement in Suzhou Garden Images

Chuanyuan Li¹, Ziyun Jiao²

School of Architecture, Sanjiang University, Nanjing, Jiangsu 210000, China¹

School of Architecture, Sanjiang University, Nanjing, Jiangsu 210000, China²

Abstract—Suzhou gardens are renowned for their unique color palettes and rich cultural significance. This study introduces a deep learning-optimized Contrast Limited Adaptive Histogram Equalization (CLAHE) method to enhance image contrast and improve color extraction accuracy in Suzhou garden images. An initial collection of 18,502 images was refined to 11,526 high-quality images from a single dataset. A pre-trained VGG16 convolutional neural network was used to extract image features, which were then employed to dynamically optimize the CLAHE parameters, thereby preserving the original color tones while enhancing contrast. The optimized CLAHE achieved significant improvements in the Structural Similarity Index (SSIM) by 24.69 percent and in the Peak Signal-to-Noise Ratio (PSNR) by 24.36 percent, and a reduction in Loss of Edge (LOE) by 36.62 percent, compared to the standard CLAHE. Additionally, enhanced structural detail and color complexity were observed. High-Resolution Network (HRNet) was utilized for semantic segmentation, enabling precise color feature extraction. K-means clustering was used to identify key color characteristics and complementary relationships among the primary and secondary colors in Suzhou gardens. A mathematical model capturing these relationships was developed to form the basis of a color palette generator, which can be applied to digital archiving, cultural preservation, aesthetic education, and virtual reality.

Keywords—Deep Learning-Optimized CLAHE; image contrast enhancement; color extraction; Suzhou gardens; VGG16; semantic segmentation

I. INTRODUCTION

Suzhou gardens are widely regarded as quintessential examples of Chinese classical garden design, embodying rich cultural and historical values. Zhang and Lian [1] describe these gardens as masterpieces that harmonize architecture, water bodies, and vegetation, reflecting cultural ethos across dynasties [2]. Jiang et al. [3] emphasize their role as cultural heritage sites illustrating aesthetic principles and socio-economic changes from the Tang to Qing Dynasties. He and Chu [4] further highlight the significance of both tangible and intangible heritage values in contemporary urban development.

However, digitally preserving the visual authenticity of these heritage sites presents significant challenges. Variations in lighting conditions across different images can lead to inconsistent color representation and contrast, complicating accurate analysis and preservation efforts. Moreover, existing color extraction methods often fail to capture the full spectrum of colors inherent in the intricate designs of Suzhou gardens, resulting in incomplete analyses that do not fully reflect the gardens' aesthetic and cultural richness.

Nallaperumal et al. [5] note difficulties in maintaining visual fidelity, while Kulkarni et al. [6] observe that color

extraction methods struggle to capture the diverse color ranges in complex environments like Suzhou gardens due to shading, lighting variations, and color shifts. Additionally, Chen and Gu [7] point out that many current studies emphasize individual color properties rather than conducting comprehensive color analyses, limiting our understanding of the full color spectrum that contributes to the gardens' aesthetic and cultural essence.

To address these issues, we propose an optimized Contrast Limited Adaptive Histogram Equalization (CLAHE) method enhanced by deep learning techniques. Traditional CLAHE relies on fixed parameter settings, which may not be optimal for the diverse and complex images of Suzhou gardens [8]. By leveraging VGG16, a deep convolutional neural network, we dynamically optimize CLAHE parameters—specifically the Clip Limit and Tile Grid Size—based on high-level image feature extraction [9]. This optimization allows CLAHE to adaptively enhance contrast while preserving original color tones, addressing the limitations of fixed parameter selection.

Furthermore, we incorporate High-Resolution Network (HRNet) for semantic segmentation to isolate garden-related elements from background noise, thereby refining color feature extraction [10].

This study advances digital heritage preservation and sustainable design by introducing a deep learning-optimized CLAHE method for color enhancement in Suzhou garden images. Enhanced color accuracy facilitates digital archiving and cultural preservation while promoting the integration of traditional aesthetics into sustainable design practices. These contributions provide valuable insights for eco-friendly applications in cultural conservation and modern design.

The main contributions of this study are summarized as follows:

1) *Deep learning-enhanced image enhancement*: We develop a novel method that dynamically optimizes CLAHE parameters using VGG16, significantly improving contrast and color preservation in Suzhou garden images.

2) *Advanced semantic segmentation*: We incorporate HRNet for precise segmentation of garden-related features, reducing noise and enhancing the accuracy of color extraction.

3) *Color clustering analysis*: Using K-means clustering in Lab color space, we identify primary and secondary color characteristics, uncovering complementary color relationships unique to Suzhou garden aesthetics.

4) *Digital preservation and design applications*: We create a color palette generator based on the identified color

relationships, providing practical tools for digital archiving, cultural preservation, aesthetic education, and virtual reality applications.

This paper is organized as follows: Section II presents an overview of related work, focusing on the traditional CLAHE method and advancements in semantic segmentation and color extraction techniques. Section III elaborates on the research methodology, including the optimization of CLAHE parameters using deep learning, semantic segmentation with HRNet, and color clustering. Section IV discusses the experimental setup, results, and analysis. Finally, Section V concludes with the implications of this study, its limitations, and potential future directions.

II. OVERVIEW OF RELATED WORK

A. CLAHE Color Correction Technique

Contrast Limited Adaptive Histogram Equalization (CLAHE) is an image processing technique designed to enhance local contrast, thereby improving overall image quality. Unlike conventional methods such as Global Histogram Equalization (GHE), Gamma Correction, and Retinex algorithms, which apply uniform adjustments across the entire image, CLAHE operates on small sections independently, providing optimal representation for each region with greater efficiency.

CLAHE has been widely adopted across various fields of image processing, demonstrating its effectiveness in numerous applications. For instance, Kim et al. [11] combined CLAHE with Retinex to improve color uniformity while reducing image interference, significantly enhancing image quality. In medical semantic segmentation, Nizamani et al. [12] showed that CLAHE can significantly improve segmentation accuracy. Additionally, CLAHE has been utilized as a preprocessing step in Convolutional Neural Networks (CNNs) to enhance the accuracy of identifying agricultural diseases, as demonstrated by Sayyid [13].

Further advancements in CLAHE have focused on noise suppression and detail enhancement in various imaging tasks, leading to superior performance [14]. Similarly, Soniminde and Biradar [15] applied CLAHE in multi-scale image fusion, resulting in improved image clarity and contrast. Its application has extended to enhancing complex images, as shown by Karthikha and Jamal [16]. In low-light conditions, Yuan et al. [17] utilized CLAHE to increase target detection accuracy. Ren and Xu [18] developed an improved CLAHE algorithm for enhancing dot-matrix invisible code images, effectively improving contrast in low-quality images. He et al. [19] applied CLAHE to low-illumination image processing in shield tunnels, achieving remarkable results and showcasing CLAHE's versatility in image enhancement tasks.

Despite its widespread adoption, traditional CLAHE methods are often hindered by fixed parameter settings that do not account for diverse lighting conditions and complex color distributions, particularly in culturally significant images like those of Suzhou gardens. Recent studies by Rahman et al. [20], [21], [22], [23], [24] have proposed advanced image enhancement models that adaptively address uneven illumination, noise suppression, and color preservation. These works highlight the

importance of leveraging techniques like multiscale decomposition, Retinex models, and dynamic parameter optimization to handle diverse imaging scenarios effectively.

Inspired by these approaches, our study introduces a novel method that leverages VGG16, a deep convolutional neural network, to dynamically optimize CLAHE parameters. By utilizing VGG16 for high-level feature extraction, our method adjusts CLAHE's Clip Limit and Tile Grid Size based on each image's unique characteristics. This deep learning-based optimization addresses the challenge of parameter selection in CLAHE, allowing it to adaptively enhance contrast while preserving original color tones. This approach is particularly advantageous for processing complex scenes, such as those found in Suzhou gardens.

B. Semantic Segmentation and Color Extraction

High-Resolution Network (HRNet) is a robust deep neural network architecture tailored for semantic segmentation, excelling in maintaining high-resolution representations while integrating multi-scale features. Enhancements such as attention mechanisms have significantly improved HRNet's segmentation accuracy, as demonstrated by Lai [25] in breast ultrasound imaging and Jin et al. [26] in landslide segmentation from remote sensing data. Liu et al. [27] utilized HRNet's superior localization to capture intricate details in retinal vessel images by introducing deformable convolutions, while Yan et al. [9] improved semantic segmentation with a boundary detail enhancement module. Kim et al. [28] further enhanced HRNet's effectiveness across various datasets through attention modules, and Sadeghi et al. [29] confirmed HRNet's superiority in high-resolution semantic segmentation through comparative analyses.

Following segmentation, K-means clustering is employed for color extraction due to its effectiveness in identifying dominant colors by minimizing the distance between data points and cluster centroids. Zhu et al. [30] demonstrated K-means' effectiveness in cultural heritage analysis by clustering colors in traditional Yi costumes. Kristanto et al. [31] enhanced segmentation accuracy in microbial images by combining K-means with Gabor filters for texture and color feature extraction. Jardim et al. [32] utilized K-means with the watershed algorithm for complex segmentation tasks, while Abernathy and Celebi [33] developed an enhanced online K-means algorithm that improved color quantization performance through incremental processing and better initialization. Bhuvanya and Kavitha [34] integrated K-means with other clustering techniques to advance image feature extraction and classification accuracy. Additionally, Kalaivani and Vimaladevi [35] improved endmember extraction in hyperspectral images by leveraging the relationship between K-means and the Pixel Purity Index, showcasing its versatility across various image analysis domains.

Integrating optimized CLAHE for color correction, HRNet for precise semantic segmentation, and K-means for effective color clustering enhances the accuracy of color extraction. This composite approach provides a solid foundation for digitally preserving the heritage of Suzhou gardens through improved color extraction techniques, enabling detailed analysis and accurate representation of their unique color palettes.

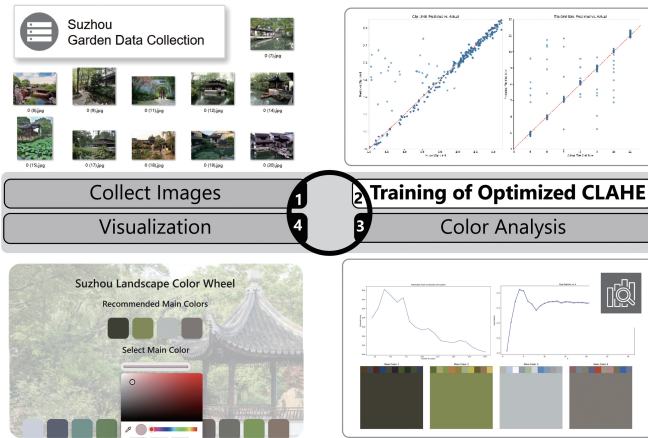


Fig. 1. Methodological roadmap.

III. RESEARCH METHODOLOGY

The methodological roadmap of this study is shown in Fig. 1.

This study integrates an optimized Contrast Limited Adaptive Histogram Equalization (CLAHE) method with a High-Resolution Network (HRNet) and K-means clustering to enhance contrast and color extraction in Suzhou garden images. To address lighting variations and incomplete color analyses, the optimized CLAHE is dynamically refined using VGG16 for effective contrast adjustment, while HRNet is employed for multi-scale semantic segmentation. K-means clustering is then applied to the segmented images to identify key color patterns and relationships.

A. Training of Optimized CLAHE

CLAHE's performance critically depends on its parameters: Clip Limit and Tile Grid Size. The Clip Limit controls maximum local contrast, reducing noise amplification, while the Tile Grid Size determines the level of local detail by segmenting the image into blocks. Traditional regression-based methods [36] have optimized these parameters; however, this study employs a deep learning-based approach for more adaptive enhancement. For the discrete Tile Grid Size, we treated optimization as a classification problem with 13 classes, corresponding to Tile Grid Sizes ranging from 8 to 32 in increments of 2. This allows the model to predict the most suitable Tile Grid Size category for each image effectively. The continuous Clip Limit is predicted using a linear activation function for fine-grained adjustments.

1) *Role of VGG-16 in parameter optimization:* VGG16, renowned for its deep convolutional architecture and effective feature extraction [37], is employed to capture high-level image features such as brightness, contrast, and fine-grained textures characteristic of Suzhou garden images. Leveraging pre-trained weights from extensive training on large datasets like ImageNet, VGG16 facilitates efficient transfer learning, enabling the model to generalize effectively across diverse image types while minimizing the need for extensive retraining.

VGG16 was chosen for its simplicity and proven effectiveness in feature extraction tasks. Compared to more recent

architectures like ResNet or EfficientNet, VGG16 offers a balanced depth and computational efficiency, making it ideal for our parameter optimization without introducing excessive complexity. Its robust feature representation from ImageNet pre-training generalizes well to various garden images.

2) *Feature extraction and parameter selection:* The VGG16 model processes each image to extract high-dimensional features, which serve as inputs for optimizing CLAHE parameters. These features are passed through a global average pooling layer to reduce dimensionality, ensuring computational efficiency while retaining essential information:

$$f_{VGG} = \text{GlobalAveragePooling2D}(\text{VGG16}(x)) \quad (1)$$

Image contrast is quantified by calculating a brightness histogram and contrast ratio:

$$l_h = \frac{\text{calcHist}([Y], [0], \text{None}, [256], [0, 256])}{\sum_{i=0}^{255} \text{calcHist}([Y], [0], \text{None}, [256], [0, 256])_i} \quad (2)$$

$$\text{contrast} = \frac{\text{std}(Y)}{\text{mean}(Y)} \quad (3)$$

To enhance dataset diversity and improve model robustness, a series of data augmentation techniques were employed:

- **Rotations:** Random rotations within $\pm 20^\circ$ to simulate diverse perspectives and improve spatial feature recognition.
- **Flipping:** Horizontal and vertical flips, each applied with a probability of 50%, enhancing the model's robustness to symmetric structures.
- **Brightness and Contrast Adjustments:** Random changes within $\pm 20\%$ to account for lighting variations.
- **Scaling:** Random resizing between 80% and 120% of the original image dimensions to accommodate scale diversity.
- **Noise Addition:** Gaussian noise was applied to simulate real-world interference and improve noise tolerance.

These augmentation techniques were specifically designed to address the unique visual complexity and dynamic conditions of Suzhou garden images. Experimental results revealed an improvement of over 10% in validation accuracy when augmentation was applied, demonstrating its critical role in enhancing model performance.

3) *Model construction and training:* Fig. 2 illustrates the workflow of the model training and evaluation process. It begins with input data (images) that undergo data preparation, including train-validation splitting and data augmentation. The model initialization uses the VGG16 architecture with random weight initialization. In the training loop, processes such as optimization, forward and backpropagation, learning rate reduction, and early stopping are applied. Once trained, the

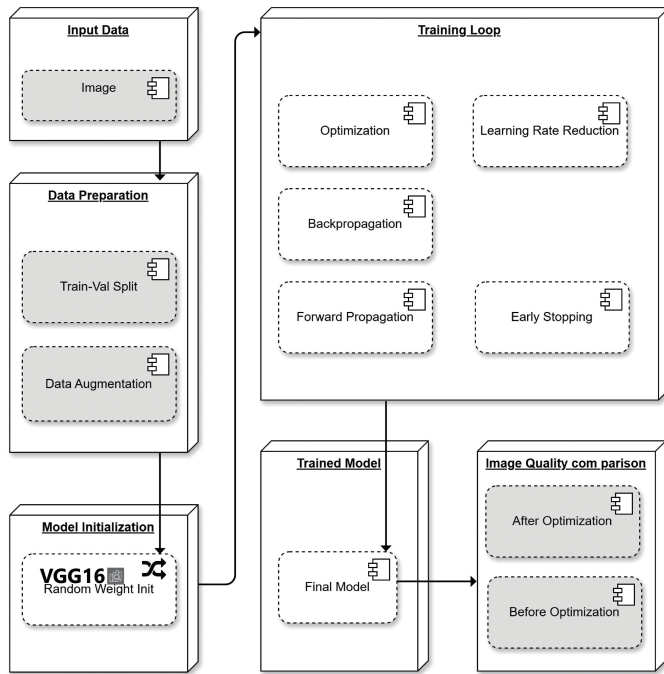


Fig. 2. Model training and evaluation workflow.

final model is evaluated by comparing image quality before and after optimization.

The model architecture comprises an input layer followed by fully connected layers to reduce the dimensionality of the feature space:

$$x_{i+1} = \text{ReLU}(\text{Dense}(x_i, \text{units} = n)) \quad (4)$$

Residual connections are incorporated to prevent gradient vanishing:

$$x_{\text{new}} = \text{add}([x_{\text{prev}}, \text{Dense}(x_{\text{prev}}, 512, \text{'relu'})]) \quad (5)$$

Using Early Stopping and ReduceLRonPlateau, the model outputs continuous predictions for optimized Clip Limit and Tile Grid Size:

$$\text{clip_limit_output} = \text{Dense}(1, \text{activation} = \text{'linear'})(x) \quad (6)$$

$$\text{tile_grid_size_output} = \text{Dense}(13, \text{'softmax'})(x) \quad (7)$$

The neural network was trained over 200 epochs with a batch size of 64, utilizing 80% of the data for training and 20% for validation. After VGG16-based feature extraction, the network architecture included fully connected layers with batch normalization and dropout regularization to ensure stability during training. Residual connections were employed to retain

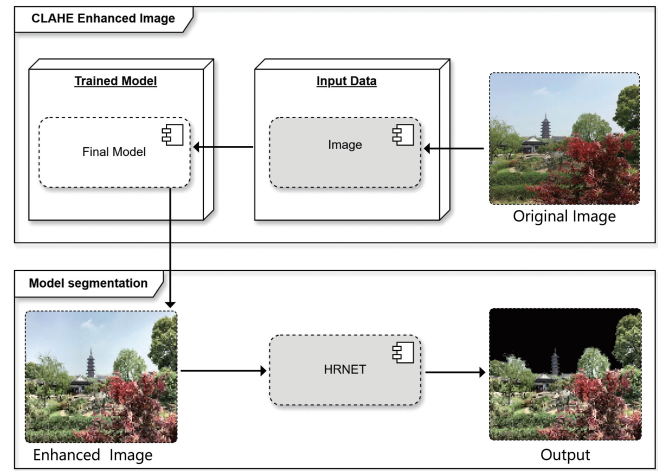


Fig. 3. HRNet flowchart.

essential information across layers, particularly at the 512-dimensional layer. This enhances gradient flow and improves learning efficiency.

The Adam optimizer was used with an initial learning rate of 0.001, which was dynamically adjusted using ReduceLRonPlateau based on the root mean squared error (RMSE) of the validation loss for the outputs. Early Stopping was applied with a patience of 20 epochs to prevent overfitting, restoring the best model weights.

B. Application of HRNet in Semantic Segmentation

HRNet is applied to CLAHE-optimized images for multi-scale feature extraction, preserving high-resolution details. Four parallel convolutional branches process features at varying scales, which are then fused for refined segmentation:

$$F_{\text{fusion}} = \sum_{i=1}^N \alpha_i \cdot F_i \quad (8)$$

The fused output enables precise identification of relevant garden regions, enhancing the accuracy of color feature extraction. Final segmentation is defined as:

$$Y_{\perp}^* = \text{argmax}(\text{softmax}(F_{\text{fusion}})) \quad (9)$$

To improve segmentation accuracy, we applied morphological operations to remove small non-garden-related elements such as sky regions and transient objects like people and cars. Additionally, connected component analysis was performed to retain only the largest contiguous garden regions, ensuring the exclusion of irrelevant areas. The HRNet flowchart is shown in Fig. 3.

C. Color Clustering and Analysis

The segmented RGB images are converted to Lab color space for better perceptual uniformity in color representation:

$$\begin{aligned} L &= 116 \cdot f\left(\frac{Y}{Y_n}\right) - 16, \\ a &= 500 \cdot \left(f\left(\frac{X}{X_n}\right) - f\left(\frac{Y}{Y_n}\right)\right), \\ b &= 200 \cdot \left(f\left(\frac{Y}{Y_n}\right) - f\left(\frac{Z}{Z_n}\right)\right) \end{aligned} \quad (10)$$

K-means clustering identifies primary and secondary colors, measuring distances using Euclidean metrics:

$$\text{Distance}(x, y) = \sqrt{\sum_{i=1}^n (x_i - y_i)^2} \quad (11)$$

Cluster centers are updated iteratively, with Euclidean distance determining dominant color clusters:

$$\mu_j = \frac{1}{n_j} \sum_{i=1}^{n_j} x_i \quad (12)$$

The distance between primary and secondary colors is calculated as:

$$\text{distance} = \sqrt{(L_1 - L_2)^2 + (a_1 - a_2)^2 + (b_1 - b_2)^2} \quad (13)$$

Linear regression is then applied to model color relationships:

$$\begin{aligned} Y &= \beta_0 + \beta_1 \cdot \text{MC } L + \beta_2 \cdot \text{MC } a + \beta_3 \cdot \text{MC } b \\ &+ \beta_4 \cdot \text{SC } L + \beta_5 \cdot \text{SC } a + \beta_6 \cdot \text{SC } b \end{aligned} \quad (14)$$

D. Validation and Visualization of Cluster Numbers

The optimal number of clusters is validated using Gap Statistic and Silhouette Score for robust clustering results. Principal Component Analysis (PCA) reduces color data dimensionality to visualize clusters effectively:

$$X_{\text{pca}} = X \cdot V_k \quad (15)$$

PCA-reduced color data undergoes K-means clustering to form primary and secondary color clusters, providing a structured analysis of color distributions in Suzhou garden images.

IV. EXPERIMENTS AND RESULTS

A. Experimental Setup

1) Optimized CLAHE processing:

a) *Suzhou garden data collection:* An automated function was developed to collect images from the internet, specifically targeting names associated with famous classical gardens or landmarks in Suzhou. The selection criteria required that these sites be recognized as World Cultural Heritage sites. These include “Canglang Pavilion,” “Huanxiu Mountain Villa,” “Lingering Garden,” “Couple’s Retreat Garden,” “Lion Grove Garden,” “Retreat and Reflection Garden,” “Garden of the Master of the Nets,” “Art Garden,” and “Humble Administrator’s Garden.” Additionally, the keywords “Classical gardens of Suzhou,” “Suzhou Garden,” and “Suzhou Classical Gardens” were used as supplements. Based on these search terms, images were collected from Baidu Images, resulting in a total of 18,502 images. The original image data are shown in Table I.

TABLE I. ORIGINAL IMAGE DATA

Keywords	Number of Pictures
Classical Gardens of Suzhou	352
Suzhou Garden	145
Canglang Pavilion	1758
Huanxiu Mountain Villa	1263
Lingering Garden	1853
Couple’s Retreat Garden	1581
Lion Grove Garden	1508
Classical Suzhou Gardens	1623
Suzhou Yuanlin	1862
Retreat and Reflection Garden	1380
Garden of the Master of the Nets	1755
Art Garden	1595
Humble Administrator’s Garden	1827

An Average Hash (AHash) algorithm was employed to identify and remove duplicate images from the collected dataset by computing the hash value for each image and deleting any identical photos. The formula for calculating the average hash is:

$$\text{average_hash} = \sum_{i=0}^n 2^i \cdot I(v_i > \text{mean}) \quad (16)$$

Following this, all images were manually reviewed to remove any non-Suzhou garden-related photos from the dataset. After this refinement process, the final number of preprocessed images was 11,526.

b) *Training and evaluation of optimized CLAHE:* The processed images of Suzhou gardens underwent necessary preprocessing steps before model training. The model was trained using the formulas provided in Eq. (1) to (7) and evaluated on a validation set. The evaluation process involved tracking changes in loss and error metrics throughout the training process and assessing regression performance using metrics such as Mean Squared Error (MSE) and R-squared (R^2).

c) *Comparison of predicted and actual values:* For the Clip Limit, most data points align closely with the red dashed line, indicating that the model achieves high predictive

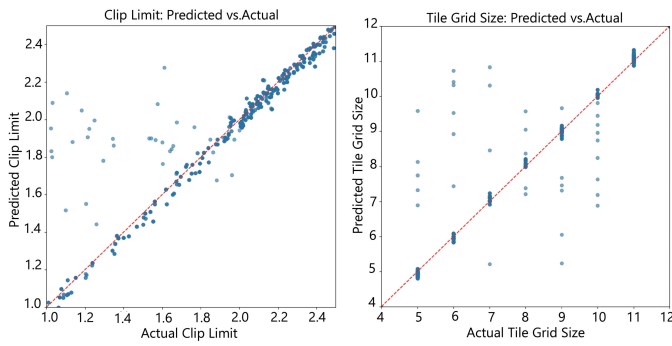


Fig. 4. Comparison of predicted value and actual value.

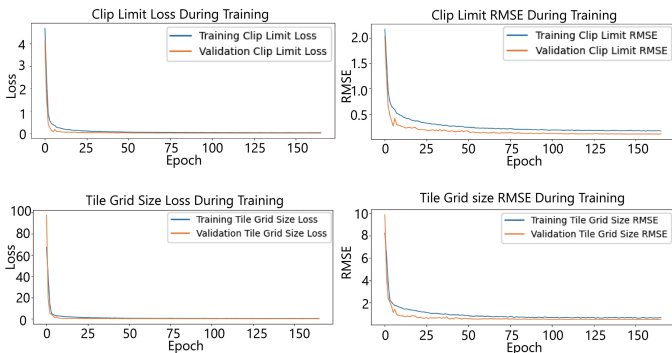


Fig. 5. Training history chart.

accuracy in the majority of cases. A few data points exhibit significant deviations, suggesting that the model may struggle with predictions under certain extreme conditions or specific scenarios. For the Tile Grid Size, the predicted values generally follow the trend of the actual values, though some deviations are noted at higher grid sizes. Despite these outliers, they are relatively rare, indicating that the model’s predictions are accurate in most situations. The analysis data is shown in Fig. 4.

d) Training history chart analysis: The training and validation loss, along with Root Mean Squared Error (RMSE), decreased rapidly during the initial stages of training and gradually stabilized, indicating that the model effectively learned the data features early on and converged progressively. The application of data augmentation techniques further contributed to minimizing overfitting and improving generalization. Notably, rotations and flips enhanced the model’s ability to generalize across diverse spatial features, while brightness and contrast adjustments improved its robustness to varying lighting conditions. The Training History information is shown in Fig. 5.

The model demonstrates strong performance in predicting the clip_limit parameter, achieving minimal prediction error and exhibiting a concentrated distribution of predictions, reflecting its robust generalization capability. While the prediction of the tile_grid_size parameter is generally good, it exhibits some limitations at larger grid sizes, suggesting areas for potential optimization in future work.

e) Comparison of CLAHE and optimized CLAHE: To objectively evaluate the performance of the optimized CLAHE method against the standard CLAHE, we applied three key image quality metrics: Structural Similarity Index (SSIM), Peak Signal-to-Noise Ratio (PSNR), and Loss of Edge (LOE). These metrics were calculated by comparing the CLAHE-enhanced images with the original images in the dataset.

SSIM measures similarity between two images by considering luminance, contrast, and structural details, where higher values indicate better structural preservation. PSNR, on the other hand, quantifies the ratio between the maximum possible signal power and the noise power; higher PSNR values imply better image quality and less noise. LOE evaluates the preservation of edge details in the images, where lower values indicate better edge retention.

The average SSIM, PSNR, and LOE values for all images were computed for both the standard CLAHE and Optimized CLAHE methods, as shown in Table II.

TABLE II. AVERAGE SSIM, PSNR, AND LOE VALUES FOR STANDARD AND OPTIMIZED CLAHE

Metric	Standard CLAHE	Optimized CLAHE	Improvement (%)
SSIM	0.4437	0.5532	+24.69%
PSNR (dB)	13.22	16.45	+24.36%
LOE	0.2314	0.1466	-36.62%

The results indicate that Optimized CLAHE achieved significant improvements over standard CLAHE, with a 24.69% increase in SSIM (from 0.4437 to 0.5532), a 24.36% improvement in PSNR (from 13.22 dB to 16.45 dB), and a 36.62% reduction in LOE (from 0.2314 to 0.1466). This demonstrates that Optimized CLAHE not only enhances contrast but also better preserves structural integrity and significantly reduces edge loss, thereby maintaining critical image details.

Fig. 6 illustrates overall performance comparisons for SSIM, PSNR, and LOE metrics. These enhanced metrics confirm that Optimized CLAHE contributes to more vivid and accurate color representation in the images, capturing the intricate details and richness of Suzhou gardens.

The evaluation results strongly suggest that the Optimized CLAHE model provides superior performance, making it a promising approach for applications requiring high-quality image enhancement.

2) HRNet Processing and Color Extraction: After applying the Optimized CLAHE processing to all images, semantic segmentation was performed using Eq. (8) and (9) to remove non-garden-related elements such as people and cars. To ensure the accuracy of color extraction, the sky was excluded before proceeding to subsequent steps.

When executing the calculations according to Eq. (10) to (12), the maximum number of clusters generated by the algorithm for each image was limited to 30. All extracted color data were converted into a DataFrame format and saved. The generated data includes the LAB values of the primary and secondary colors for each image, and Table III provides information about an image named “Image1”.

Eq. (13) and (14) generate the color clustering formulas as follows:

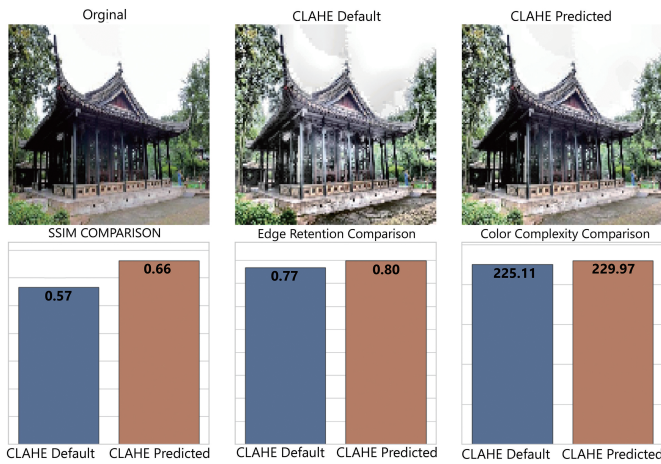


Fig. 6. Performance comparison of CLAHE and enhanced CLAHE.

TABLE III. COLOR CARD LAB VALUES - IMAGE 1

L	a	b	Ratio
34.1446	0.4313	9.8101	0.0463
87.6003	-0.2872	-10.7976	0.0334
17.2502	3.0355	2.4672	0.0717
64.0184	3.5201	14.0537	0.0256
56.8409	-23.9924	34.4455	0.0158
97.1075	-1.0001	-1.1957	0.0837
53.0612	10.1856	21.9371	0.0180
76.0309	3.2525	-0.4037	0.0474
37.9928	3.8353	-6.3526	0.0169
57.2163	2.3148	-4.1065	0.0217
46.6206	5.3030	3.2603	0.0373
86.9956	3.5583	3.1048	0.0817
44.1516	0.0378	12.3873	0.0390
40.4602	9.3195	15.2071	0.0118
55.0158	2.8220	5.9573	0.0556
68.0085	7.8041	27.5084	0.0391

$$Y = 35.78 + 0.19 \cdot MCL + 0.002 \cdot MCa - 0.28 \cdot MCb - 0.22 \cdot SCL + 0.10 \cdot SCa + 0.46 \cdot SCb \quad (17)$$

The range of Y is [0.0,163.32] and its data distribution is shown in the figure below. To control the range, the values between the 25th and 75th percentiles are selected as the

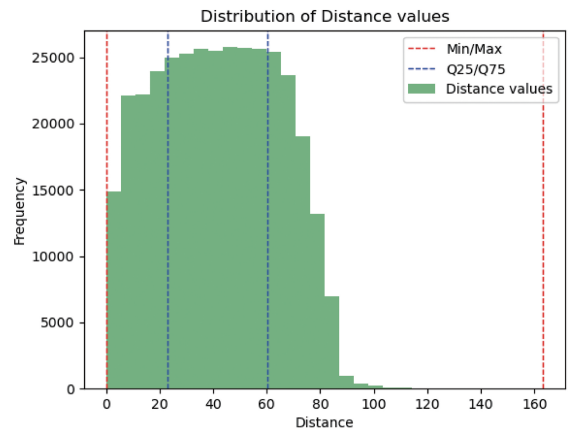


Fig. 7. Y Value range definition.

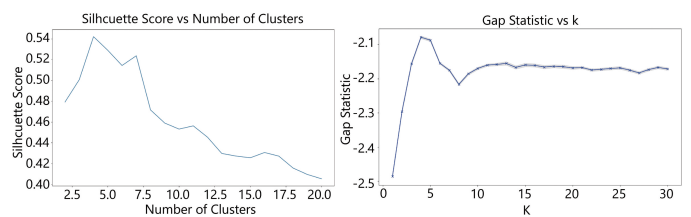


Fig. 8. Cluster quantity analysis.

controlled range for Y. The final range of Y is [22.84, 60.38]. The relevant information is shown in Fig. 7.

The Gap Statistic and Silhouette Score were compared for different numbers of clusters, revealing that the optimal number of clusters is 4. This suggests that the clustering effect is best when the number of primary colors is 4. The Cluster Quantity Analysis is illustrated in Fig. 8.

Using Eq. (15), the reduced-dimensional color data was clustered using the K-means algorithm to identify the main color cluster centers (primary colors). For each primary color, the corresponding secondary colors were further clustered using the K-means algorithm, with the cluster centers selected to represent these secondary colors. To aid in visualization, the maximum number of clusters for secondary colors corresponding to each primary color was limited to 10, ensuring clarity and manageability in the resulting visual representation. Information called “Color Card LAB Values” is shown in Tables IV, V, VI, and VII. Each support color represents a secondary color that complements the main color within its group, contributing to the overall color harmony observed in Suzhou gardens.

The final visualization image generated by this process is shown in Fig. 9.

B. Results and Analysis

Using Eq. (17), our analysis reveals that the color design of Suzhou classical gardens exhibits a complementary relationship in terms of lightness (L) and the blue-yellow channel (b). Specifically, there is a positive or negative correlation between “Main Color L” and “Support Color L” as well as between

TABLE IV. COLOR CARD LAB VALUES - GROUP 1

Color Result Group 1			
Color Type	L	a	b
Support Color 1	28.84	8.37	22.32
Support Color 2	30.20	-1.83	-3.60
Support Color 3	22.73	21.81	11.61
Support Color 4	26.59	4.82	-35.18
Support Color 5	29.95	-2.03	8.03
Support Color 6	15.79	4.41	-0.66
Support Color 7	33.93	-15.91	21.87
Support Color 8	19.57	-6.58	10.27
Support Color 9	32.30	-14.70	15.67
Support Color 10	26.51	0.44	-10.59
Main Color 1	26.77	-1.55	7.34

TABLE V. COLOR CARD LAB VALUES - GROUP 2

Color Result Group 2			
Color Type	L	a	b
Support Color 1	43.19	-14.52	31.60
Support Color 2	71.68	-8.94	37.19
Support Color 3	62.60	-24.40	47.16
Support Color 4	59.29	23.75	44.69
Support Color 5	56.44	-1.80	49.71
Support Color 6	73.83	-13.11	24.92
Support Color 7	80.02	-12.28	67.12
Support Color 8	39.95	-0.67	31.99
Support Color 9	53.12	3.85	29.67
Support Color 10	81.91	-1.46	57.86
Main Color 2	57.56	-16.58	35.54

“Main Color b” and “Support Color L.” The Euclidean distance of color differences predominantly falls within the range of [22.84, 60.38], which is considered the “harmony” standard in garden color design.

This harmony is achieved through the subtle control of contrast in secondary colors, reflecting the traditional philosophy of “harmony between humans and nature” and the concept of “calm and introspection.” Suzhou gardens create a rich visual experience by uniting the stability of primary colors with the diversity of secondary colors. The study also indicates that secondary colors, particularly those in the blue-yellow spectrum (such as tones of sunlight, water surfaces, and autumn leaves), significantly influence the overall visual experience and play a crucial role in determining the color difference distance (Y). In contrast, the influence of the main color’s a value is found to be minimal.

Building on these findings, we developed a color palette generator program designed to automatically create color schemes that align with the design principles of Suzhou gardens. This tool provides practical applications for heritage

TABLE VI. COLOR CARD LAB VALUES - GROUP 3

Color Result Group 3			
Color Type	L	a	b
Support Color 1	77.76	-2.90	6.01
Support Color 2	84.69	-0.38	-14.41
Support Color 3	98.18	-0.23	0.43
Support Color 4	67.34	-0.59	-8.70
Support Color 5	77.32	-12.04	17.55
Support Color 6	88.17	-0.26	-0.14
Support Color 7	62.07	10.53	-50.65
Support Color 8	66.76	-2.14	-18.09
Support Color 9	68.37	-1.52	3.36
Support Color 10	74.33	0.15	-4.63
Main Color 3	80.49	-1.61	0.24

TABLE VII. COLOR CARD LAB VALUES - GROUP 4

Color Result Group 4			
Color Type	L	a	b
Support Color 1	47.20	16.61	12.50
Support Color 2	54.80	-1.07	-5.90
Support Color 3	53.24	-1.60	13.72
Support Color 4	42.84	6.98	-24.07
Support Color 5	46.77	54.44	47.14
Support Color 6	65.06	-1.26	17.93
Support Color 7	63.90	17.13	11.22
Support Color 8	47.68	1.44	18.59
Support Color 9	44.59	14.93	-53.98
Support Color 10	50.82	4.07	-14.29
Main Color 4	51.47	0.99	5.99

preservation, garden design, aesthetic education, and virtual reality. The development program is shown in Fig. 10.

C. Limitations

1) *Clustering method:* While K-means clustering effectively identified dominant color clusters, its assumption of spherical clusters may not capture the nuanced color variations inherent in Suzhou gardens. Alternative methods like Gaussian Mixture Models (GMM) or DBSCAN could potentially model more complex color distributions.

2) *Parameter optimization robustness:* The deep learning-based optimization of CLAHE parameters, though effective, may require further refinement to handle extreme lighting conditions or highly complex scenes beyond the current dataset.

3) *Dataset diversity:* The dataset, while extensive, may still lack certain variations in garden scenes, such as seasonal changes or rare architectural elements, potentially limiting the universality of the model.

D. Future Work

Future research could address these limitations by exploring more sophisticated clustering techniques and improving the robustness of parameter optimization. Expanding the dataset to include a wider variety of garden scenes and conditions would further enhance the model’s generalizability. Additionally, integrating reinforcement learning for real-time parameter adjustments and exploring end-to-end deep learning models for simultaneous enhancement and color extraction present promising directions. Applying this methodology to other culturally significant heritage sites could also validate its versatility and effectiveness across diverse contexts.

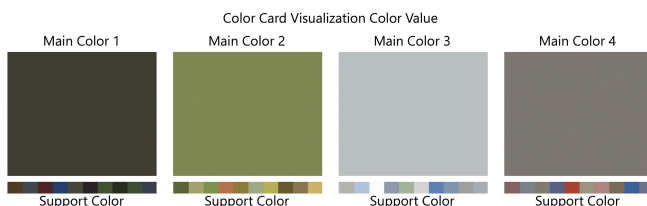


Fig. 9. Color card visualization of color value.

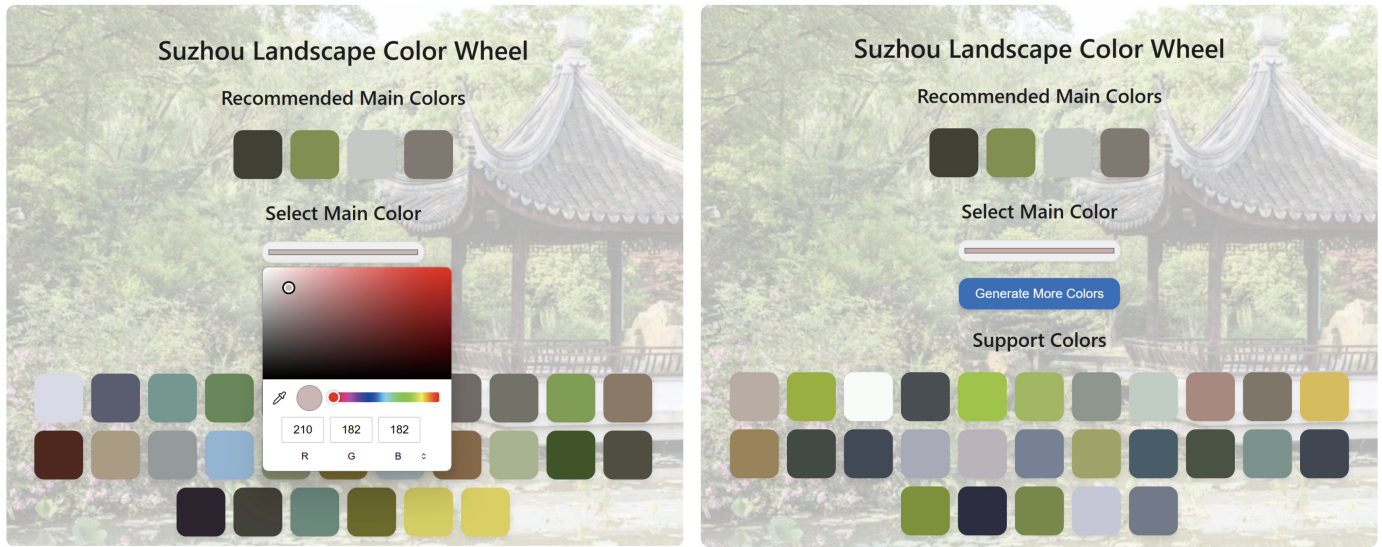


Fig. 10. Color palette generator development program

V. CONCLUSION

This study explored the integration of an optimized Contrast Limited Adaptive Histogram Equalization (CLAHE) algorithm for enhancing image contrast and accurately extracting colors from images of Suzhou gardens. The findings demonstrated the potential of this approach to improve the visualization of fine details, preserve structural integrity, and capture a richer spectrum of colors in heritage images. Specifically, the optimized CLAHE showed a 24.69% improvement in Structural Similarity Index (SSIM), a 24.36% increase in Peak Signal-to-Noise Ratio (PSNR), and a 36.62% reduction in Loss of Edge (LOE), alongside enhanced color complexity and edge preservation.

The use of VGG16 for dynamic parameter optimization allowed CLAHE to adapt to each image's unique characteristics, ensuring consistent enhancement across varied lighting and shading conditions. High-Resolution Network (HRNet) further refined the segmentation process, isolating garden-related elements and enhancing the accuracy of color feature extraction. K-means clustering effectively identified primary and secondary color clusters, revealing complementary color relationships that align with the traditional aesthetics of Suzhou gardens.

Despite these advancements, some limitations remain. The reliance on the K-means algorithm for color clustering, while effective for basic categorizations, may not fully capture the nuanced color variations characteristic of Suzhou gardens. Additionally, while deep learning (DL) was utilized to optimize CLAHE parameters, further refinement is needed to make this approach robust across diverse imaging scenarios. Future work could explore more sophisticated clustering techniques, such as Gaussian Mixture Models (GMMs) or advanced deep learning methods, to provide a more comprehensive understanding of color relationships in heritage contexts.

The findings of this study have several implications for future research. First, there is potential to expand the application of this method beyond Suzhou gardens to other complex

imaging scenarios, such as urban landscapes, natural reserves, or historic façades. Such explorations could validate the generalizability and utility of the proposed techniques across diverse cultural heritage sites. Second, further advancements in adaptive parameter optimization for CLAHE, possibly using reinforcement learning or other machine learning approaches, could enhance the adaptability and effectiveness of image enhancement techniques in real-time applications.

Overall, this study contributes to the field of cultural heritage preservation by demonstrating the value of integrating advanced image processing techniques with deep learning algorithms to enhance the analysis and documentation of classical Chinese gardens. By addressing current limitations and exploring new research directions, future studies can further refine these methods and expand their applicability, ultimately advancing the digital preservation and understanding of cultural heritage.

This work lays a foundation for more sophisticated tools that not only preserve the aesthetic qualities of heritage sites but also enhance their accessibility and comprehensibility for future generations.

FINANCIAL DISCLOSURE

National Natural Science Foundation Project (51408337). Universities' philosophy and Social Sciences Research Projects in Jiangsu Province (KZ2022017)

CONFLICT OF INTEREST

The authors declare no potential conflict of interests.

CODE AND DATA AVAILABILITY

The code related to this study is publicly available on GitHub at: https://github.com/andrew849039/optimized_clahe

REFERENCES

- [1] Y. Zhang and Z. Lian, "Research on the distribution and scale evolution of Suzhou gardens under the urbanization process from the Tang to the Qing dynasty," *Land*, vol. 10, no. 3, p. 281, 2021.
- [2] X. Yi, "The tangible and intangible value of the Suzhou classical gardens," in *Proceedings of the 16th ICOMOS General Assembly and International Symposium 'Finding the Spirit of Place—Between the Tangible and the Intangible'*, p. 29, Quebec, QC, Canada, 2008.
- [3] J. Jiang, et al., "Urban heritage conservation and modern urban development from the perspective of the historic urban landscape approach: A case study of Suzhou," *Land*, vol. 11, no. 8, p. 1251, 2022.
- [4] Q. He and C.-H. H. Chu, "A new shadow removal method for color images," in *International Conference Paper*, 2013.
- [5] K. Nallaperumal, et al., "An analysis of suitable color space for visually plausible shadow-free scene reconstruction from single image," in *2013 IEEE International Conference on Computational Intelligence and Computing Research*, 2013.
- [6] K. Kulkarni, P. Patil, and S. G. Kanakaraddi, "Multi-modal colour extraction using deep learning techniques," in *2022 Fourth International Conference on Emerging Research in Electronics, Computer Science and Technology (ICERECT)*, 2022.
- [7] Y. Chen and F. Gu, "Quantitative analysis of traditional Chinese color," *BioResources*, vol. 18, no. 3, 2023.
- [8] S. Sahu, et al., "An approach for de-noising and contrast enhancement of retinal fundus image using CLAHE," *Optics Laser Technology*, vol. 110, pp. 87–98, 2019.
- [9] G. Yan, et al., "Enhancing building segmentation in remote sensing images: Advanced multi-scale boundary refinement with mbr-HRNet," *Remote Sensing*, vol. 15, no. 15, p. 3766, 2023.
- [10] J. Wang, et al., "Deep high-resolution representation learning for visual recognition," *IEEE Transactions on Pattern Analysis and Machine Intelligence*, vol. 43, no. 10, pp. 3349–3364, 2020.
- [11] Y.-J. Kim, D.-M. Son, and S.-H. Lee, "Retinex jointed multiscale CLAHE model for HDR image tone compression," *Mathematics*, vol. 12, no. 10, p. 1541, 2024.
- [12] A. H. Nizamani, et al., "Advance brain tumor segmentation using feature fusion methods with deep U-Net model with CNN for MRI data," *Journal of King Saud University-Computer and Information Sciences*, vol. 35, no. 9, p. 101793, 2023.
- [13] M. F. N. Sayyid, "Klasifikasi penyakit daun jagung menggunakan metode CNN dengan image processing HE dan CLAHE," *Jurnal Teknik Informatika dan Teknologi Informasi*, vol. 4, no. 1, pp. 86–95, 2024.
- [14] X. Zhao, et al., "Application and analysis of medical image processing based on improved CLAHE," in *International Conference on Artificial Intelligence in China*, Springer Nature Singapore, Singapore, 2023.
- [15] N. V. Soniminde and M. Biradar, "Improving wavelet-based image fusion with weighted average of high boost and CLAHE," in *2024 IEEE International Students' Conference on Electrical, Electronics and Computer Science (SCEECS)*, IEEE, 2024.
- [16] R. Karthikha and D. N. Jamal, "Enhancing colonoscopy image quality with CLAHE in the Gastrolab dataset," in *2023 3rd International Conference on Innovative Mechanisms for Industry Applications (ICIMIA)*, IEEE, 2023.
- [17] Z. Yuan, et al., "CLAHE-based low-light image enhancement for robust object detection in overhead power transmission system," *IEEE Transactions on Power Delivery*, vol. 38, no. 3, pp. 2240–2243, 2023.
- [18] M. Ren and J. Xu, "An improved CLAHE image enhancement algorithm for dot matrix invisible code," in *Eighth International Conference on Electronic Technology and Information Science (ICETIS 2023)*, vol. 12715, SPIE, 2023.
- [19] Z. He, et al., "Multi-scale fusion for image enhancement in shield tunneling: A combined MSRCR and CLAHE approach," *Measurement Science and Technology*, vol. 35, no. 5, p. 056112, 2024.
- [20] Z. Rahman, Y.-F. Pu, M. Aamir, S. Wali, and Y. Guan, "Efficient image enhancement model for correcting uneven illumination images," *IEEE Access*, vol. 8, pp. 109038–109053, 2020, doi: 10.1109/ACCESS.2020.3001206.
- [21] Z. Rahman, Y.-F. Pu, M. Aamir, and S. Wali, "Structure revealing of low-light images using wavelet transform based on fractional-order denoising and multiscale decomposition," *The Visual Computer*, vol. 37, no. 5, pp. 865–880, 2021.
- [22] Z. Rahman, Z. Ali, I. Khan, M. I. Uddin, Y. Guan, and Z. Hu, "Diverse image enhancer for complex underexposed image," *Journal of Electronic Imaging*, vol. 31, no. 4, p. 041213, 2022.
- [23] Z. Rahman, M. Aamir, Z. Ali, A. K. J. Saudagar, A. AlTameem, and M. Khan, "Efficient contrast adjustment and fusion method for underexposed images in industrial cyber-physical systems," *IEEE Systems Journal*, vol. 17, no. 4, pp. 5085–5096, 2023.
- [24] Z. Rahman, J. A. Bhutto, M. Aamir, Z. A. Dayo, and Y. Guan, "Exploring a radically new exponential Retinex model for multi-task environments," *Journal of King Saud University-Computer and Information Sciences*, vol. 35, no. 7, p. 101635, 2023.
- [25] S. Lai, "GMS-uHRNet: A global multi-scale spatial U-HRNet for breast ultrasound semantic segmentation," in *International Conference on Image, Signal Processing, and Pattern Recognition (ISPP 2024)*, vol. 13180, SPIE, 2024.
- [26] Y. Jin, X. Liu, and X. Huang, "EMR-HRNet: A multi-scale feature fusion network for landslide segmentation from remote sensing images," *Sensors*, vol. 24, no. 11, p. 3677, 2024.
- [27] J. Liu, et al., "HRD-net: High resolution segmentation network with adaptive learning ability of retinal vessel features," *Computers in Biology and Medicine*, vol. 173, p. 108295, 2024.
- [28] J.-S. Kim, et al., "E-HRNet: Enhanced semantic segmentation using squeeze and excitation," *Electronics*, vol. 12, no. 17, p. 3619, 2023.
- [29] N. Sadeghi, et al., "Comparing the semantic segmentation of high-resolution images using deep convolutional networks: SegNet, HRNet, CSE-HRNet and RCA-FCN," *Journal of Information Systems and Telecommunication (JIST)*, vol. 4, no. 44, p. 359, 2023.
- [30] H. Zhu, et al., "Application of K-means algorithm in Yi clothing color," in *International Conference on Internet of Things and Machine Learning (IoTML 2021)*, vol. 12174, SPIE, 2022.
- [31] S. P. Kristanto, L. Hakim, and D. Yusuf, "K-means clustering segmentation on water microbial image with color and texture feature extraction," *Building of Informatics, Technology and Science (BITS)*, vol. 4, no. 3, pp. 1317–1324, 2022.
- [32] S. Jardim, J. António, and C. Mora, "Graphical image region extraction with K-means clustering and watershed," *Journal of Imaging*, vol. 8, no. 6, p. 163, 2022.
- [33] A. Abernathy and M. E. Celebi, "The incremental online K-means clustering algorithm and its application to color quantization," *Expert Systems with Applications*, vol. 207, p. 117927, 2022.
- [34] R. Bhuvanya and M. Kavitha, "Image clustering and feature extraction by utilizing an improvised unsupervised learning approach," *Cybernetics and Information Technologies*, vol. 23, no. 2, pp. 3–19, 2023.
- [35] S. Kalaivani and M. R. Vimaladevi, "Enhancing endmember extraction using K-means clustering and pixel purity index," in *2023 2nd International Conference on Vision Towards Emerging Trends in Communication and Networking Technologies (ViTECoN)*, IEEE, 2023.
- [36] G. F. C. Campos, et al., "Machine learning hyperparameter selection for Contrast Limited Adaptive Histogram Equalization," *EURASIP Journal on Image and Video Processing*, pp. 1–18, 2019.
- [37] K. Simonyan and A. Zisserman, "Very deep convolutional networks for large-scale image recognition," *arXiv preprint arXiv:1409.1556*, 2014.